Supporting Information

SI Materials and Methods

Cloning of *phoQ* and *phoP* in pBAD vectors. *E. coli phoQ* gene was cloned in the vector pBAD33RBS at *SacI*/*XbaI* restriction sites. The pBAD33RBS vector is derived from pBAD33 with a ribosome binding site inserted 3 bases upstream of the *SacI* site, which leads to a 9-base distance to the start codon of cloned genes. Mutants of *phoQ* were generated using Q5® site-directed mutagenesis kit (New England BioLabs) and the mutations were verified by plasmid DNA sequencing. *E. coli phoP* gene was cloned in the vector pBAD18RBS, which is derived from pBAD18 with a ribosome-binding site inserted in the same fashion as described above. A codon optimized HA tag was added to the C-terminus of *phoP* using Q5® site-directed mutagenesis kit (New England Biolabs).

Molecular dynamics (MD) simulations. PhoQ TM dimer was inserted into a 70×70 $Å^2$ palmitoyl oleoly phosphatidyl ethanolamine (POPE) membrane bilayer using CHARMM-GUI (1). The lower limit for the distance between the atoms of the peptide and the edge of the box was set to 10 Å. Na^+ and Cl^- ions were added by replacing solvent molecules to maintain the electrostatic neutrality and mimic physiological conditions with an ionic strength of 0.15 M. The system was minimized using steepest descent minimization approach and equilibrated then (Table S4). During production simulations, the system was coupled to a Nose-Hoover thermostat at 300 K with a coupling constant of 1.0 ps and to a semi-isotropic Parrinello-Rahman barostat (at 1.0 atm in the lateral *X*-*Y* plain and 1.0 atm in the axial *Z* direction) with a coupling constant of 5.0 ps and compressibility of 4.5×10^{-5} bar^{-1}. To enable the 2 fs integration time step, all hydrogen bonds were constrained using the LINCS (2) algorithm. The cut-off distance for the electrostatic and Lennard-Jones forces was set to 12 Å. Each simulated trajectory corresponds to 1 μs, with snapshots saved every 20 ps. The last 800 ns of trajectories were used for further analyses. In the subsequent step, the system was duplicated and simulated under coupling to semi-isotropic barostat at 1.25, 1.5, 1.75, 2.0, 2.25 or 2.5 atm in the lateral *X*-*Y* plain and 1.0 atm in the axial Z direction to mimic different osmolarity (3, 4). All simulations were analyzed using the GROMACS utilities (5) with PyMol (6) and custom-written scripts. The same methods and parameters were used for structure preparation and simulations of $PhoQ^{N202A}$.

Proteomic analysis. *E. coli* cell pellets were resuspended in lysis buffer containing 0.5% sodium lauroyl sarcosinate (SLS) and 100 mM ammonium bicarbonate. Cells were lysed by incubation at 95°C for 15min and sonication (Vial Tweeter, Hielscher). Cell lysates were then reduced by adding 5 mM Tris(2-caboxyethyl)phosphine and incubating at 95°C for 15 minutes followed by alkylation (10mM iodoacetamide, 30min at 25°C). Cell lysates were cleared by centrifugation and the total protein was estimated for each sample with Pierce™ BCA Protein Assay Kit (ThermoFisher Scientific). Cell lysate containing 50 μg total protein was then digested with 1 μg trypsin (Promega) overnight at 30°C in 0.5% SLS and 100 mM ammonium bicarbonate for each sample. Next, SLS was removed by precipitation with 1.5% trifluoroacetic acid (TFA) and centrifugation.

Peptides were purified using C18 microspin columns according to the manufactor's instruction (Harvard Apparatus). Purified peptides were dried, resuspended in 0.1% TFA and analyzed using liquid chromatography-mass spectrometry carried out on a Q-Exactive Plus instrument connected to an Ultimate 3000 RSLC nano with a Prowflow upgrade and a nanospray flex ion source (all Thermo Scientific). Peptide separation was performed on a reverse phase HPLC column (75 µm x 42 cm) packed in-house with C18 resin (2.4 µm, Dr. Maisch). The following separating gradient was used: 98% solvent A (0.15% formic acid) and 2% solvent B (99.85% acetonitrile, 0.15% formic acid) to 25% solvent B over 105 minutes and to 35% B for additional 35 minutes at a flow rate of 300 nl/min. The data acquisition mode was set to obtain one high resolution MS scan at a resolution of 70,000 full width at half maximum (at m/z 200) followed by MS/MS scans of the 10 most intense ions. To increase the efficiency of MS/MS attempts, the charged state screening modus was enabled to exclude unassigned and singly charged ions. The dynamic exclusion duration was set to 30 seconds. The ion accumulation time was set to 50 ms for MS and 50 ms at 17,500 resolution for MS/MS. The automatic gain control was set to $3x10^6$ for MS survey scans and $1x10^5$ for MS/MS scans.

Label-free quantification (LFQ) of the data was performed as described previously (7-9). In short, for LFQ the raw data was loaded into Progenesis (Version 2.0, Nonlinear Dynamics) and exported mgf files searched by MASCOT (Version 2.5, Matrix Science). Progenesis peptide measurement exports were then further evaluated using SafeQuant for false discovery adjustment and quality control.

SI Figure legends

Fig. S1. Transcription profiles of indicated genes after hyperosmotic treatment with 300 mM NaCl via RT-qPCR. (A) The transcription of PhoQ/PhoP regulated genes in *E. coli* strain MG1655. **(B)** The transcription of *mgtA* gene in *E. coli* MG1655, *ΔenvZ* and *ΔompR* strains. **(C)** The transcription of EnvZ/OmpR regulated genes in *E. coli* MG1655 strain. Data represent the averages of three experiments and error bars show standard deviations. .

Fig. S2. Characterizatoin of PhoQ-mediated response to osmotic upshiftes. (A) Transcriptional changes of *mgtA* gene in *E. coli ΔphoQ* strains complemented with either *E. coli phoQ* or *Salmonella phoQ* after 300 mM NaCl treatment monitored by RT-qPCR. **(B)** Expression of P_{mgtL}-GFP reporter in *E. coli* cells before or after 300 mM NaCl treatment measured by flow cytometry. **(C)** Responses of *E. coli* PhoQ mutants to osmotic upshifts. *E. coli ΔphoQ* strain was complemented with empty vector, the wild type or PhoQ mutants, as indicated. The responses were monitored using P_{mgtLA}-GFP reporter. Data represent the averages of three independent experiments and error bars show standard deviations in (A) and (C). Data represent three independent experiments in (B).

Fig. S3. Normalized activity of P_{mgtLA}-GFP reporter in the *ΔphoQ* strains expressing either the wild type or PhoQ mutants. (A) Strains were grown to OD=0.4 in Medium A supplemented with 10 mM $MgSO_4$, then treated with

300mM NaCl for 30 min. Cells were collected before (labeled as 0 mM NaCl) or after the treatment (labeled as 300 mM NaCl) and the fluorecent signals were measured and normalized to values before the NaCl stimulation for each experiment. **(B)** Strains were grown to OD=0.4 in the presence of 10 mM or 1 mM $MgSO_4$. Fluorecent signals were measured and normalized to samples grown in the presence of 10 mM magnesium . Data represent the averages of three independent experiments and error bars show standard deviations.

Fig. S4. Growth curves of *E. coli* strains in the presence of NaCl. (A) Growth difference between the wild type and *ΔphoQ* strains under different NaCl concentrations as indicated. **(B)** Growth curves of the *E. coli* wild type and deletion strains with or without 600 mM NaCl. **(C)** Growth curves of *E. coli* wild type with empty plasmid and *ΔphoQ* strain complemented with *phoQ* expressed from plasmid at 0.002% arabinose induction. Data represent three independent experiments.

Fig. S5. Overview of the input-output funciton of the PhoQ/PhoP two-component system in *E. coli* and *Salmonella*. Inputs sensed and genes regulated by the system are specified .

Fig. S6. Comparison of *E. coli* double deletion strain *ΔphoQΔiraM* to the wild type and *ΔphoQ* strains. (A) Growth curves of indicated *E. coli* strains with or without 600 mM NaCl. **(B)** The amount of RpoS *in vivo* after osmotic stress with 600 mM NaCl. Equal amounts of cells were collected at each time points for cell lysate preparation and equal amounts of cell lysate were loaded in each lane. Data represent three independent experiments.

Fig. S1.

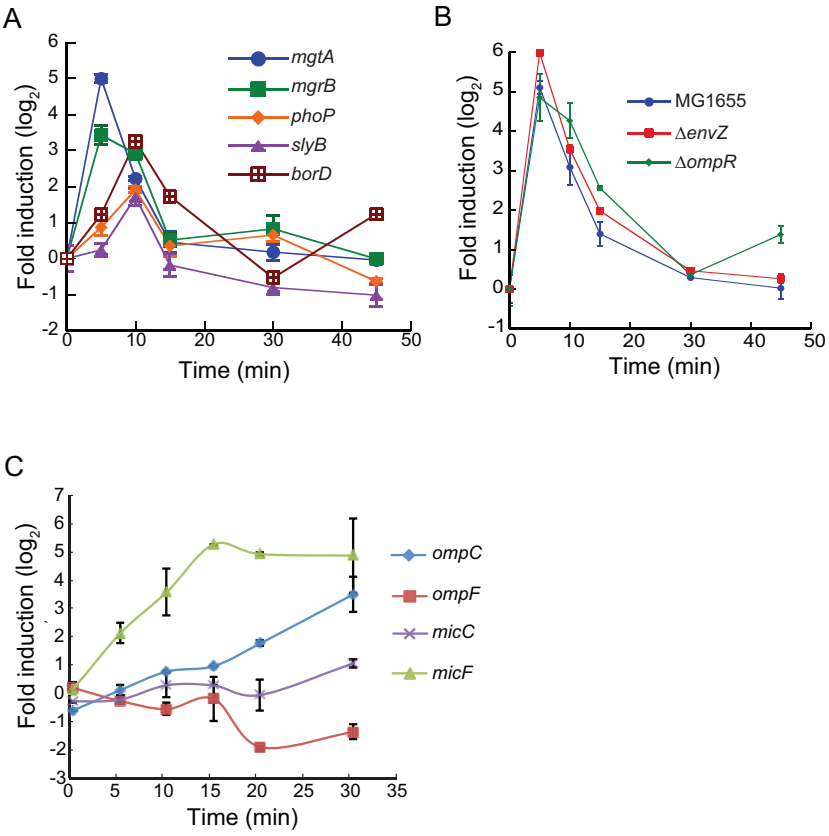
A
Fold induction (log2)
Time (min)
mgtA
mgrB
phoP
slyB
borD
B
Fold induction (log2)
Time (min)
MG1655
ΔenvZ
ΔompR
C
Fold induction (log2)
Time (min)
ompC
ompF
micC
micF

Fig. S2.

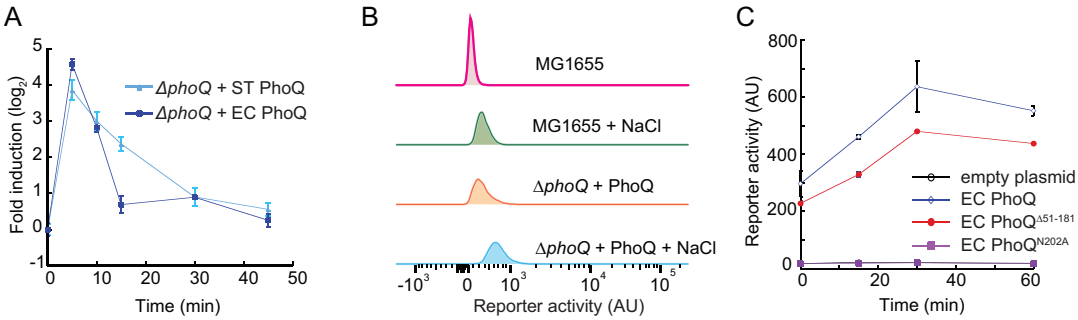
A
Fold induction (log2)
ΔphoQ + ST PhoQ
ΔphoQ + EC PhoQ
Time (min)
B
MG1655
MG1655 + NaCl
ΔphoQ + PhoQ
ΔphoQ + PhoQ + NaCl
Reporter activity (AU)
C
Reporter activity (AU)
empty plasmid
EC PhoQ
EC PhoQΔ51-181
EC PhoQN202A
Time (min)

Fig. S3.

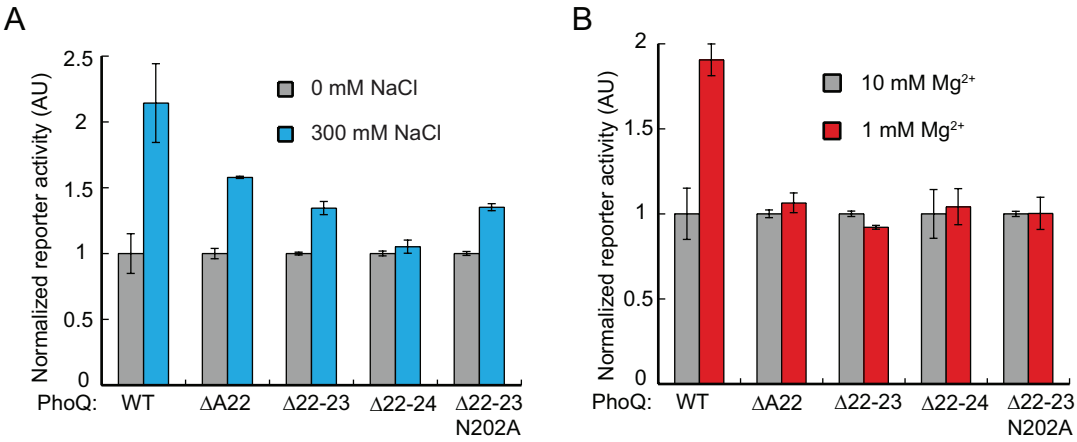
A
Normalized reporter activity (AU)
2.5
2
1.5
1
0.5
0
0 mM NaCl
300 mM NaCl
PhoQ:
WT
ΔA22
Δ22-23
Δ22-24
Δ22-23 N202A
B
Normalized reporter activity (AU)
2
1.5
1
0.5
0
10 mM Mg2+
1 mM Mg2+
PhoQ:
WT
ΔA22
Δ22-23
Δ22-24
Δ22-23 N202A

Fig. S4.

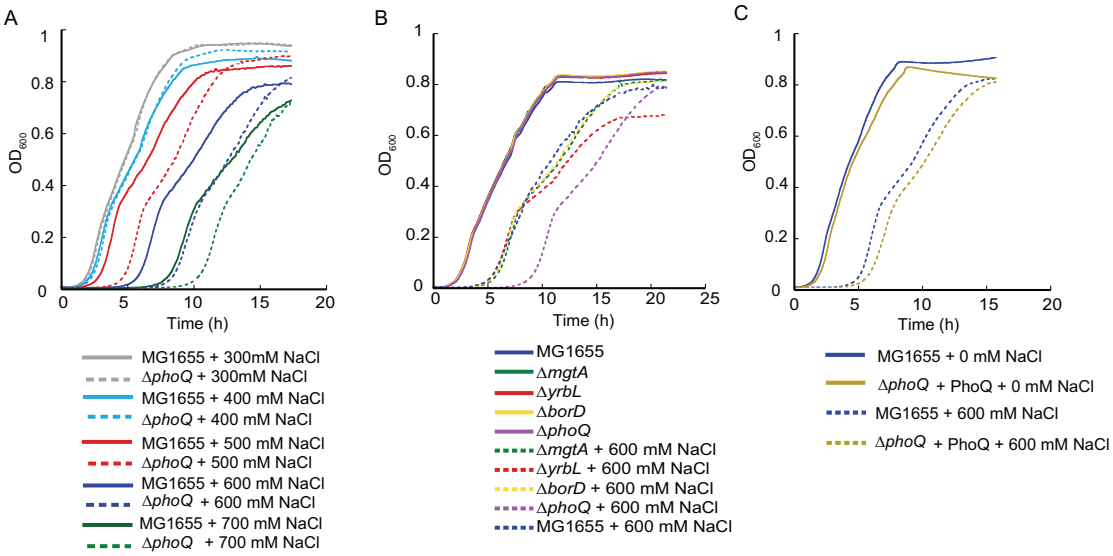
A
B
C
OD600
Time (h)
MG1655 + 300mM NaCl
ΔphoQ + 300mM NaCl
MG1655 + 400 mM NaCl
ΔphoQ + 400 mM NaCl
MG1655 + 500 mM NaCl
ΔphoQ + 500 mM NaCl
MG1655 + 600 mM NaCl
ΔphoQ + 600 mM NaCl
MG1655 + 700 mM NaCl
ΔphoQ + 700 mM NaCl
MG1655
ΔmgtA
ΔyrbL
ΔborD
ΔphoQ
ΔmgtA + 600 mM NaCl
ΔyrbL + 600 mM NaCl
ΔborD + 600 mM NaCl
ΔphoQ + 600 mM NaCl
MG1655 + 600 mM NaCl
MG1655 + 0 mM NaCl
ΔphoQ + PhoQ + 0 mM NaCl
MG1655 + 600 mM NaCl
ΔphoQ + PhoQ + 600 mM NaCl

Fig. S5.

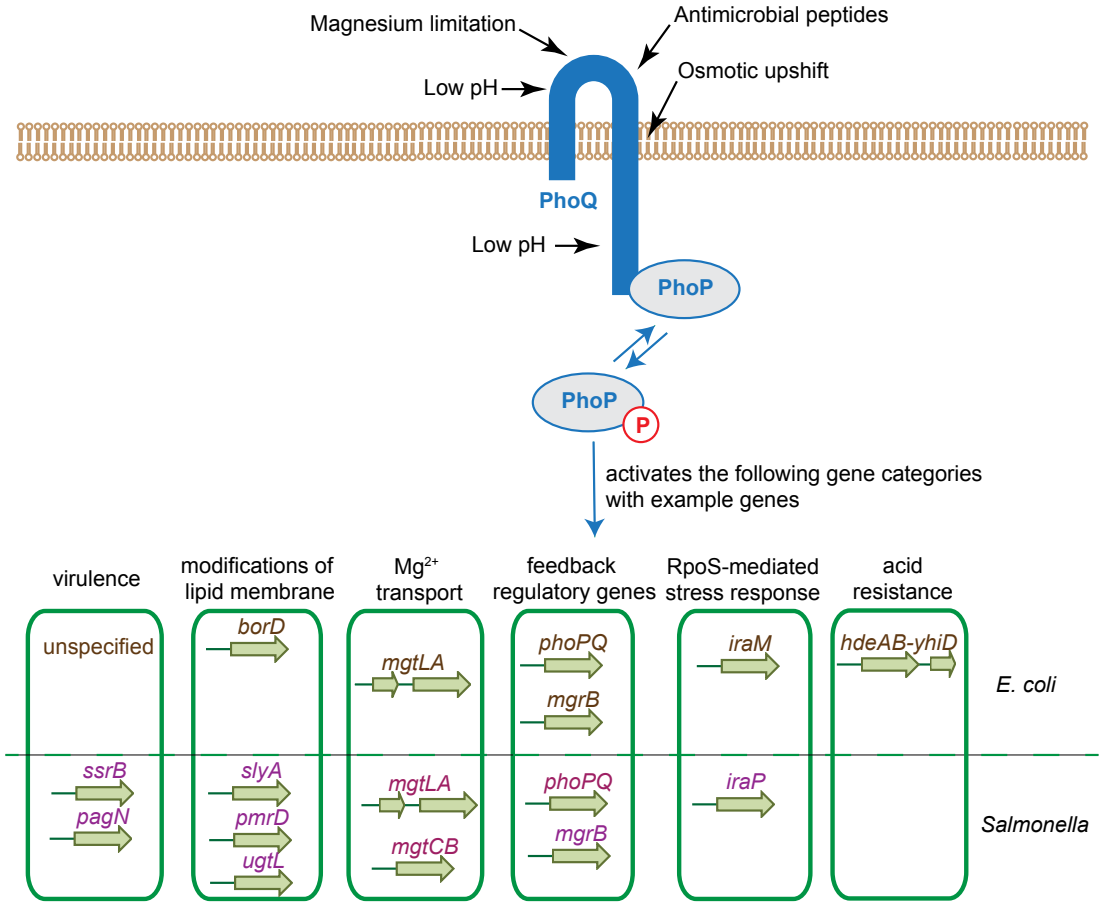
Magnesium limitation
Antimicrobial peptides
Low pH
Osmotic upshift
PhoQ
Low pH
PhoP
PhoP
P
activates the following gene categories
with example genes
virulence
modifications of lipid membrane
Mg2+ transport
feedback regulatory genes
RpoS-mediated stress response
acid resistance
unspecified
borD
mgtLA
phoPQ
mgrB
iraM
hdeAB-yhiD
E. coli
ssrB
pagN
slyA
pmrD
ugtL
mgtLA
mgtCB
phoPQ
mgrB
iraP
Salmonella

Fig. S6.

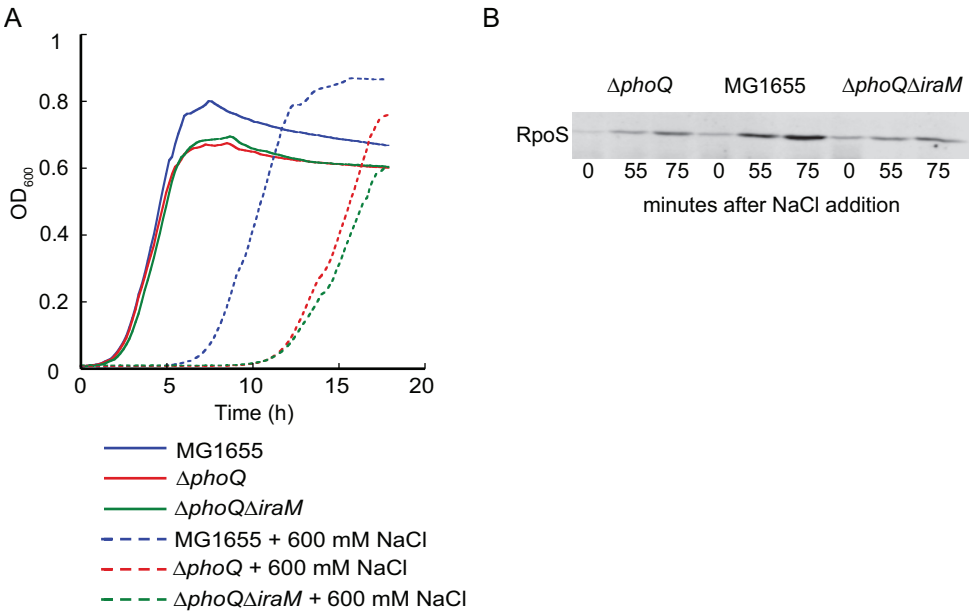
A
B
ΔphoQ
MG1655
ΔphoQΔiraM
RpoS
0 55 75 0 55 75 0 55 75
minutes after NaCl addition
OD600
Time (h)
MG1655
ΔphoQ
ΔphoQΔiraM
MG1655 + 600 mM NaCl
ΔphoQ + 600 mM NaCl
ΔphoQΔiraM + 600 mM NaCl

Table S1. List of strains with plasmids used in this study.

Strain Name	Genotype
JingY11	*MG1655*
JingY34	*MG1655 ΔmgrB*
JingY32	*MG1655 ΔmgrB pUA66 EC PmgtLA-GFP*
JingY69	*MG1655 ΔphoQ pBAD33RBS EC phoQ Δ22, pUA66 EC PmgtLA-GFP*
JingY70	*MG1655 ΔphoQ pBAD33RBS EC phoQ Δ22-23, pUA66 EC PmgtLA-GFP*
JingY71	*MG1655 ΔphoQ pBAD33RBS EC phoQ Δ22-24, pUA66 EC PmgtLA-GFP*
JingY104	*MG1655 ΔphoQ pBAD33RBS EC phoQ N202A + Δ22-23, pUA66 EC PmgtLA-GFP*
JingY27	*MG1655 ΔphoQ pBAD33RBS EC phoQ Δ51-181, pUA66 EC PmgtLA-GFP*
JingY25	*MG1655 ΔphoQ pBAD33RBS ST phoQ*
JingY17	*MG1655 ΔphoQ pBAD33RBS*
JingY28	*MG1655 ΔphoQ pBAD33RBS EC phoQ N202A, pUA66 EC PmgtLA-GFP*
JingY29	*MG1655 ΔphoQ pBAD33RBS EC phoQ, pUA66 EC PmgtLA-GFP*
JingY25	*MG1655 ΔphoQ pBAD33RBS ST phoQ*
JingY30	*MG1655 ΔphoQ pBAD33RBS, pUA66 EC PmgtLA-GFP*
JingY18	*MG1655 ΔphoQ pBAD33RBS EC phoQ*
JingY20	*MG1655 ΔphoQ pBAD33RBS EC phoQ N202A*
JingY19	*MG1655 ΔphoQ pBAD33RBS EC phoQ Δ51-181*
JingY97	*MG1655 ΔphoPQ pBAD33RBS phoPQ*
JingY100	*MG1655 ΔphoPQ pBAD33RBS phoQ*
JingY2	*MG1655 pBAD33RBS EC phoQ N202A*
JingY33	*MG1655 pUA66 EC PmgrB-GFP*
JingY31	*MG1655 pUA66 EC PmgtLA-GFP*
JingY40	*MG1655 ΔborD*
JingY21	*MG1655 ΔenvZ*
JingY16	*MG1655 ΔiraM*
JingY15	*MG1655 ΔmgrB*
JingY41	*MG1655 ΔmgtA*
JingY13	*MG1655 ΔompR*
JingY14	*MG1655 ΔphoP*
JingY12	*MG1655 ΔphoQ*
JingY6	*MG1655 ΔphoQ pUA66 EC PmgrB-GFP*
JingY10	*MG1655 ΔphoQ pUA66 EC PmgtLA-GFP*
JingY43	*MG1655 ΔproP*
JingY42	*MG1655 ΔyrbL*
JingY102	*MG1655 ΔmgrB pBAD18RBS EC phoP-HA*

Table S2. List of primers for qRT-PCR used in this study. All primers are located in the coding region of corresponding genes.

borDfw	5'-^{128}TTTCTGGAATTGGGCAGAAG^{147}-3'
borDrv	5'-^{221}ACGAATGTTTGCTGGGTTTC^{202}-3'
iraDfw	5'-^{103}TCTCCTCATTCGGCATTACC^{122}-3'
iraDrv	5'-^{204}CTGACGGCAATACCAGCTCT^{185}-3'
iraMfw	5'-^{106}TTTCTCCCTCCTGGCAGTAT^{125}-3'
iraMrv	5'-^{207}CTTGTTGAATGGTGCGATGT^{188}-3'
iraPfw	5'-^{71}CGCAGGTAGAAGCTTTGGAG^{90}-3'
iraPrv	5'-^{164}GCCCCCTCTACCTGATCAAT^{145}-3'
mgrBfw	5'-^{8}AGTTTCGATGGGTCGTTCTG^{27}-3'
mgrBrv	5'-^{89}TGATCGCACATCATGTTGAA^{70}-3'
mgtAfw	5'-^{2520}GACCGTGATCGTGATGATTG^{2539}-3'
mgtArv	5'-^{2619}CAGCCACGGGAAATAGCTTA^{2600}-3'
micCfw	5'-^{4}ATATGCCTTTATTGTCACAGATTTT^{28}-3'
micCrv	5'-^{94}GACTGTTCGGGCTTGTCTTT^{75}-3'
micFfw	5'-^{6}CATCATTAACTTTATTTATTACCGTCA^{32}-3'
micFrv	5'-^{76}AGGCATCCGGTTGAAATAGG^{57}-3'
ompCfw	5'-^{146}ATGTAGATGGCGACCAGACC^{165}-3'
ompCrv	5'-^{250}TGCCCTGGATCTGATATTCC^{231}-3'
ompFfw	5'-^{316}GCATTCGCGGGTCTTAAATA^{335}-3'
ompFrv	5'-^{416}TCTGGCAGCATATCGGTGTA^{397}-3'
phoPfw	5'-^{278}CCGGTGCTGATGATTATGTG^{297}-3'
phoPrv	5'-^{380}ATGACCTGTGAAGCCAGACC^{361}-3'
slyBfw	5'-^{144}ACGTCCGGTACAGATTCAGG^{163}-3'
slyBrv	5'-^{245}GTTCCGCCACCAACAGTATT^{226}-3'
ssrAfw	5'-^{8}ATTCTGGATTCGACGGGATT^{27}-3'
ssrArv	5'-^{105}AGTTTTCGTCGTTTGCGACT^{86}-3'
yrbLfw	5'-^{432}AGAGGTTATCCCGGTCGTCT^{451}-3'
yrbLrv	5'-^{536}TTCCATAACCGCTCTTGCTT^{517}-3'

Table S3. The proteomics data of indicated proteins in *E. coli* strains before (WT0 and *ΔphoQ*0) and after the treatment of 300 mM NaCl for 30 minutes (WT30 and *ΔphoQ*30).

Protein name	EF-G	MgtA	BorD	PhoP	SlyB
IdScore	6913.07	255.4	175.77	639.79	650.27
Nb_peptides	41	5	2	8	6
WT0	3044298448	693605	3322518	5666395	70358392
*Δpho*Q0	3024509738	22291	615299	5060579	47914710
WT30	2849077107	1112782	19048413	13496293	92939782
*Δpho*Q30	2821495590	21984	565477	7541653	46940949
CV_WT0	0.01536	0.07433	0.09065	0.07001	0.03043
CV_ *ΔphoQ*0	0.01203	0.14119	0.07118	0.01673	0.03931
CV_WT30	0.02383	0.08469	0.04320	0.02468	0.06884
CV_ *ΔphoQ*30	0.00822	0.17018	0.24079	0.06233	0.03020
Log_2 (WT30/WT0)	-0.09562	0.68198	2.51932	1.25206	0.40157
Log_2 (*ΔphoQ*30/ *ΔphoQ*0)	-0.10024	-0.02002	-0.12182	0.57558	-0.02962
p-value_(WT vs. *ΔphoQ*)	0.4670	0.0300	0.0002	0.0006	0.0014

Liquid chromatography- mass spectrometry data were analyzed with Progenesis 2.0 (Nonlinear Dynamics) for label-free quantification (LFQ). The LFQ dataset was then further evaluated by SafeQuant (7) to calculate several statistical parameters and adjust protein false discovery rate (FDR). Here a protein 1% protein FDR is used. IdScore is the sum of the Mascot ion score for the number quantified peptides (Nb_peptides). CV stands for coefficient of variation. Data represent the averages of independently processed biological triplecates.

Table S4. Equilibration protocols and changes of the restraints.

Equilibration	Duration (ns)	Accumulated time (ns)	Restraints (kcal/mol Å^2)	
			Peptide position[a]	Helix[b]
Stage 1	100	100	2000 → 500	0
Stage 2	50	150	500 → 0	0 → 500
Stage 3	50	200	0	500 → 0

a. Harmonic position restraints for all backbone atoms of PhoQ dimer peptide.
b. Restraints for the distances of nitrogen-oxygen pairs of first and last three hydrogen bonds of each main chain TM helices. The restraint potential for the PhoQ TM helices is flat bottomed between 2.8 to 3.5 Å and harmonic outside of the region.

During three equilibration processes, temperature of the system was maintained at 300 K by coupling to Berendsen thermostat with coupling constant 0.2 ps, while pressure was controlled by semi isotropic Berendsen barostat (at 1.0, 1.25, 1.5, 1.75, 2.0, 2.25, and 2.5 ATM in X-Y plain respectively and 1.0 ATM in Z direction, see Figure 1) with coupling constant 5.0 ps and compressibility of 4.5 10-5 bar-1. The time step was 2 fs in stage 1, while 1 fs in stage 2 and 3.

Table S5. An example of the RT-qPCR absolute Cq values of tmRNA (*ssrA*) during an osmotic upshift. Cells were treated with 300 mM NaCl and samples were collected at 0, 5, 10, 15, 30 and 45 minutes time points.

Well	Fluor	Target	Content	Sample	Cq
B01	SYBR	ssrA	Unkn-01	phoQ 00	16.32
B02	SYBR	ssrA	Unkn-01	phoQ 00	15.70
B03	SYBR	ssrA	Unkn-01	phoQ 00	16.28
B04	SYBR	ssrA	Unkn-02	phoQ 05	15.55
B05	SYBR	ssrA	Unkn-02	phoQ 05	16.38
B06	SYBR	ssrA	Unkn-02	phoQ 05	16.22
B07	SYBR	ssrA	Unkn-03	phoQ 10	15.87
B08	SYBR	ssrA	Unkn-03	phoQ 10	15.49
B09	SYBR	ssrA	Unkn-03	phoQ 10	15.82
B10	SYBR	ssrA	Unkn-04	phoQ 15	16.11
B11	SYBR	ssrA	Unkn-04	phoQ 15	16.12
B12	SYBR	ssrA	Unkn-04	phoQ 15	16.19
B13	SYBR	ssrA	Unkn-05	phoQ 30	15.74
B14	SYBR	ssrA	Unkn-05	phoQ 30	15.62
B15	SYBR	ssrA	Unkn-05	phoQ 30	15.44
B16	SYBR	ssrA	Unkn-06	phoQ 45	15.56
B17	SYBR	ssrA	Unkn-06	phoQ 45	16.15
B18	SYBR	ssrA	Unkn-06	phoQ 45	16.03

SI References

1. Jo S, Kim T, Iyer VG, & Im W (2008) CHARMM-GUI: A web-based graphical user interface for CHARMM. *Journal of Computational Chemistry* 29(11):1859-1865.
2. Hess B, Bekker H, Berendsen HJC, & Fraaije JGEM (1997) LINCS: A linear constraint solver for molecular simulations. *Journal of Computational Chemistry* 18(12):1463-1472.
3. Xie JY, Ding GH, & Karttunen M (2014) Molecular dynamics simulations of lipid membranes with lateral force: rupture and dynamic properties. *Biochim Biophys Acta* 1838(3):994-1002.
4. Muddana HS, Gullapalli RR, Manias E, & Butler PJ (2011) Atomistic simulation of lipid and DiI dynamics in membrane bilayers under tension. *Phys Chem Chem Phys* 13(4):1368-1378.
5. Abraham MJ*, et al.* (2015) GROMACS: High performance molecular simulations through multi-level parallelism from laptops to supercomputers. *SoftwareX* 1–2:19-25.

6. LLC S (2010) The PyMOL molecular graphics system. Version 1.5.0.4.
7. Glatter T, Ahrne E, & Schmidt A (2015) Comparison of Different Sample Preparation Protocols Reveals Lysis Buffer-Specific Extraction Biases in Gram-Negative Bacteria and Human Cells. *J Proteome Res* 14(11):4472-4485.
8. Glatter T*, et al.* (2012) Large-scale quantitative assessment of different in-solution protein digestion protocols reveals superior cleavage efficiency of tandem Lys-C/trypsin proteolysis over trypsin digestion. *J Proteome Res* 11(11):5145-5156.
9. Ahrne E, Molzahn L, Glatter T, & Schmidt A (2013) Critical assessment of proteome-wide label-free absolute abundance estimation strategies. *Proteomics* 13(17):2567-2578.